$+ \sigma^*_Z$) if $\rho^* = -0.89$. For protonated hemiacetals, RCH_2OH^+-CH_2OH, we use $pK_a = -5.01 - 1.8\sigma^*_R$ or $pK_a = -3.79 - 0.89\sigma^*_R$.

For cationic tetrahedral intermediates ionizing to give zwitterions, $R(Z)C(OH_3^+)(OH)$, we use $pK_a = 10.32 - 1.32(\sigma^*_R + \sigma^*_Z)$.[12] For ionization of the CH_2OH group in hemiacetals, or protonated hemiacetals, we estimate ρ^* using a fall-off factor of 0.36.[44] This leads to $pK_a = 8.93 - 0.17\sigma^*_R$ for RCH_2OH^+-CH_2OH and to $pK_a = 13.31 - 0.17\sigma^*_R$ for RCH_2OCH_2OH. For neutral tetrahedral intermediates we use the Hine equation.[23]

Supplementary Material Available: Table III, limiting pK_a values for the reactions considered (3 pages). Ordering information is given on any current masthead page.

(44) Barlin, G. B.; Perrin, D. D. *Q. Rev., Chem. Soc.* **1966**, *20*, 75.
(45) Bell, R. P. *Adv. Phys. Org. Chem.* **1966**, *4*, 1.
(46) Le Henaff, P. *Bull. Soc. Chim. Fr.* **1968**, 4687.
(47) Bell, R. P.; Evans, P. G. *Proc. R. Soc. London, Ser. A* **1966**, *291*, 297.
(48) Kurz, J. L. *J. Am. Chem. Soc.* **1967**, *89*, 3524.
(49) Bell, R. B.; Rand, M. H.; Wynne-Jones, K. M. A. *Trans. Faraday Soc.* **1956**, *52*, 1093.
(50) Guthrie, J. P.; Cullimore, P. A., *Can. J. Chem.*, in press.
(51) Salmi, E. J.; Suonpaa, J. *Chem. Ber.* **1940**, *73*, 1126.
(52) Barthel, J.; Bader, G.; Schmeer, G. *Z. Phys. Chem. (Frankfurt am Main)* **1968**, *62*, 63.
(53) Skrabal, A.; Zahorka, A. *Monatsh. Chem.* **1929**, *53–54*, 562.
(54) Fairclough, R. A.; Hinshelwood, G. N. *J. Chem. Soc.* **1937**, 538.
(55) Blackburn, G. M.; Jencks, W. P. *J. Am. Chem. Soc.* **1968**, *90*, 2638.
(56) Kresge, A. J.; Sagatys, D. S.; Chen, H. L. *J. Am. Chem. Soc.* **1977**, *99*, 7228.
(57) Jencks, W. P.; Carriuolo, J. *J. Am. Chem. Soc.* **1961**, *83*, 1743.
(58) Kirsch, J. F.; Jencks, W. P. *J. Am. Chem. Soc.* **1964**, *86*, 837.
(59) Cohen, A. O.; Marcus, R. A. *J. Phys. Chem.* **1968**, *72*, 4249. Marcus, R. A. *J. Am. Chem. Soc.* **1969**, *91*, 7224. *Annu. Rev. Phys. Chem.* **1964**, *15*, 155, and references cited therein.
(60) Hine, J. *J. Am. Chem. Soc.* **1971**, *93*, 3701.
(61) Necessarily, an "intermediate" with a lifetime of less than one molecular vibration cannot be said to exist as a discrete species, and there cannot be a stepwise path via such an intermediate. Our treatment leads to the conclusion that even intermediates with finite lifetimes can be avoided by concerted paths if the reaction coordinate diagrams permit.
(62) Recently[63] it has been shown that the hydrolysis of substituted benzaldehyde acetals is subject to general acid catalysis. Unfortunately, the equilibrium constant for oxocarbonium ion is not known for any of the benzaldehydes, so we cannot apply our method.
(63) Jensen, J. L.; Herold, L. R.; Lenz, P. A.; Trusty, S.; Sergei, V.; Bell, K.; Rogers, P. *J. Am. Chem. Soc.* **1979**, *101*, 4672.

Nanosecond Time-Resolved Fluorescence of Phototautomeric Lumichrome[1]

Jung Do Choi, Robert D. Fugate, and Pill-Soon Song*[2]

Contribution from the Department of Chemistry, Texas Tech University, Lubbock, Texas 79409.
Received January 18, 1980

Abstract: Lumichrome (7,8-dimethylalloxazine) emits two fluorescence bands with maxima at 440 and 540 nm in pyridine–dioxane and acetic acid–ethanol mixtures. The nanosecond time-resolved fluorescence of lumichrome shows a fast growth of the latter upon excitation of lumichrome with a 2-ns pulse, as the result of proton transfer from N_1 to N_{10} during the lifetime of the lumichrome singlet. The rate depends on the concentration of general base (pyridine) and bifunctional catalysts (acetic acid). From pH-dependence study of the nanosecond time-resolved fluorescence spectra of lumichrome in aqueous solution, the photodissociation of the N_1 proton appears to be slower than the phototautomerism in pyridine–dioxane or acetic acid–ethanol mixtures. The temperature dependence of the phototautomerism of lumichrome showed an efficient proton transfer from N_1 to N_{10} at temperatures higher than 100 K.

Introduction

Lumichrome (7,8-dimethylalloxazine, **1**), a flavin tautomer, exhibits two fluorescence emission maxima, 440 and 540 nm, in pyridine–dioxane mixture.[3] These fluorescence spectra are attributed to emission from the excited states of lumichrome (**1**) and its tautomer flavin (**2**). The latter is formed during the

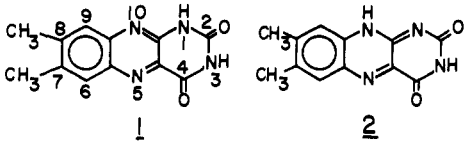

1 **2**

excited-state lifetime of the former, catalyzed by pyridine which facilitates transfer of a proton from the N_1 to the N_{10} position.[3,4]

Similar phototautomerism of **1** occurs in an acetic acid–ethanol mixture, in which the acid functions as a bifunctional catalyst for the excited-state proton transfer.[3] Various substituted alloxazines display phototautomerism.[5] In aqueous alloxazine solutions, multiple excited-state equilibria occur as the result of tautomeric and ionization equilibria.[5,6]

In the previous work mentioned above,[3,5] the phototautomerism was indirectly measured in terms of steady-state fluorescence and it was possible neither to extract rate constants nor to discriminate between the phototautomerism and photodissociation of **1**. Although the phase-modulation fluorescence lifetime data were consistent with the steady-state fluorescence studies,[4] it was not possible to elucidate the kinetics and mechanism of phototautomerism of **1** in detail. In the present paper, we report nanosecond time-resolved fluorescence measurements of the phototautomerism of **1** in order to more fully describe the excited-state behavior of **1**.

Experimental Section

Materials. Lumichrome (7,8-dimethylalloxazine, **1**) was obtained and purified as described previously,[3,7] and as a gift from Professor J. Koziol. Spectroquality solvents (*p*-dioxane and ethanol) were obtained from Matheson Coleman and Bell and U.S. Industries, respectively. Acetic acid (Ultrex grade, 99.9%) was purchased from J. T. Baker Chemical Co. Pyridine, spectroquality, was obtained from Matheson Coleman and Bell.

(1) Supported by the Robert A. Welch Foundation (D-182) and the National Science Foundation (PCM75-05001).
(2) To whom correspondence should be addressed.
(3) Song, P.-S.; Sun, M.; Koziolowa, A.; Koziol, J. *J. Am. Chem. Soc.* **1974**, *96*, 4319.
(4) Fugate, R. D.; Song, P.-S. *Photochem. Photobiol.* **1976**, *24*, 479.
(5) Koziolowa, A. *Photochem. Photobiol.* **1979**, *29*, 459.
(6) Müller, F.; Dudley, K. H. *Helv. Chim. Acta* **1971**, *54*, 1487.
(7) Sun, M.; Moore, T. A.; Song, P.-S. *J. Am. Chem. Soc.* **1972**, *94*, 1730.

0002-7863/80/1502-5293$01.00/0

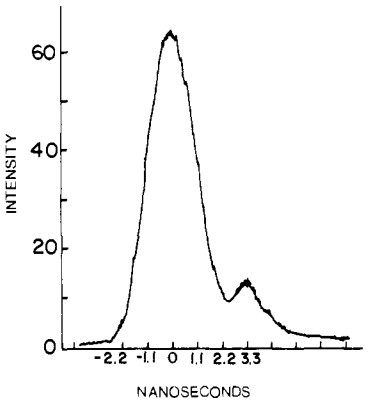

Figure 1. A typical intensity–time profile of the Optitron NR-11 nanosecond optical pulse radiator (from N_2 plasma discharge) used for recording time-resolved fluorescence spectra of lumichrome. The 0-ns origin designates the pulse maximum.

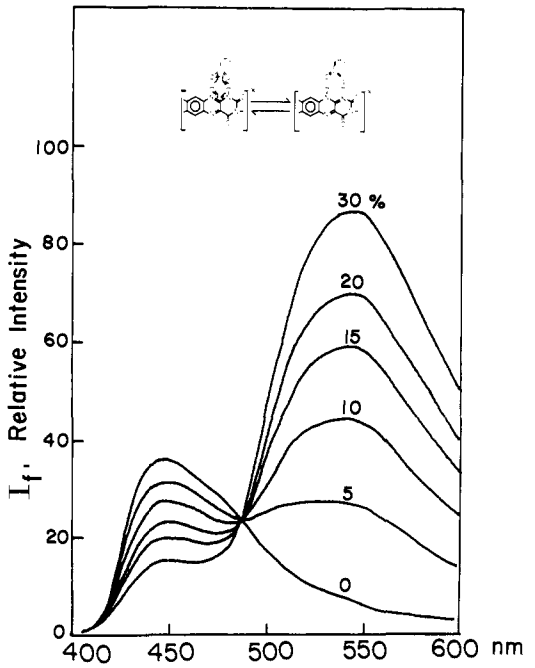

Figure 2. The corrected fluorescence spectra of lumichrome ($A_{385} \sim 0.8$) in ethanol as a function of acetic acid concentration at 298 K, $\lambda_{ex} \sim 395$ nm. The emission maxima at 448 and 545 nm are due to the phototautomeric equilibrium shown at the top inset (see ref 3 for the phototautomeric equilibrium of lumichrome).

Methods. Steady-state fluorescence measurements were carried out on a Perkin-Elmer MPF 44B spectrofluorometer equipped with a DCSU-2 differential corrected spectra unit. Fluorescence yields (ϕ) were estimated by integrating emission bands and by referring to known values.[5] Fluorescence decays were measured on an SLM-480 subnanosecond phase-modulation fluorometer[4] and a nanosecond time-resolved spectrofluorometer constructed in this laboratory, as described below. In the latter method of fluorescence decay measurements, the data were treated on the Texas Tech University computer interfaced to the spectrofluorometer in order to effectively subtract out the effects of lamp flash variation on the sample decay curves (e.g., see Figure 1 for the lamp intensity–time profile). For this purpose, we have utilized the phase-plane method of Demas and Adamson.[9]

The nanosecond time-resolved spectrofluorometer is essentially the same design as that described earlier.[8] It uses a PAR dual channel Model 162 boxcar averager with Model 163 sampling integrators fitted with Tektronix S-2 sampling heads (75-ps sampling width). The light source is a free-running Optitron Model NR-11 nitrogen discharge lamp with a repetition rate of 5 kHz and fwhm of about 2 ns. The detector consists of a Bausch & Lomb high-intensity monochromator and an EMI 9817B photomultiplier tube. Time-resolved spectra are generated by setting the boxcar at a fixed aperture (time window) with respect to the lamp intensity peak and then scanning the monochromator and X–Y recorder simultaneously across the wavelength region of interest. A complete set of time-resolved spectra can then be generated by advancing the aperture and rescanning the spectrum. In our opinion, this method is simpler and more direct than recording a series of decay curves at various wavelengths and then utilizing these to construct the time-resolved spectrum.

(8) Badea, M. G.; Georghiou, S. *Rev. Sci. Instrum.* **1976**, *47*, 314.
(9) Demas, J. N.; Adamson, A. W. *J. Phys. Chem.* **1971**, *75*, 2463.

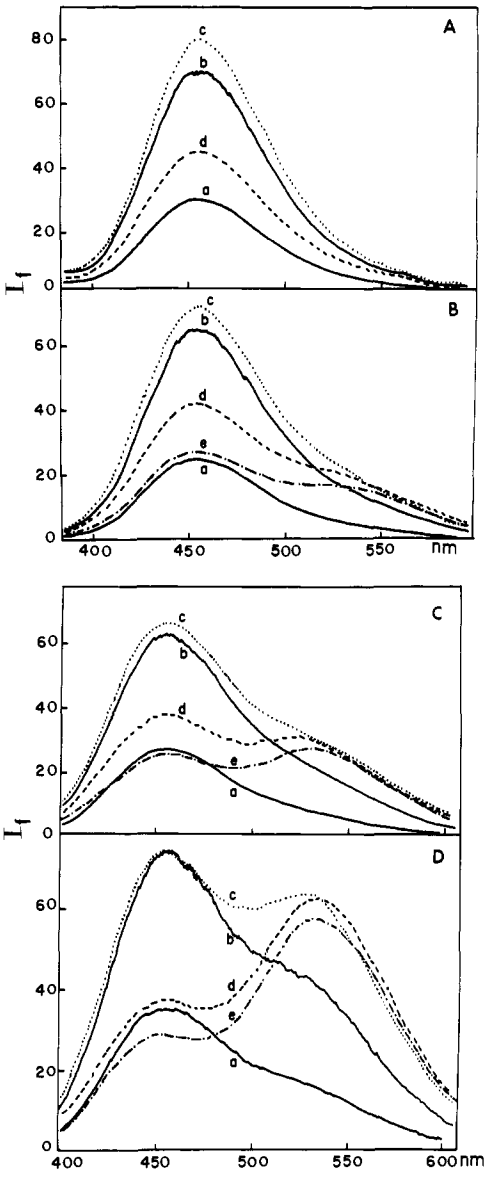

Figure 3. The time-resolved fluorescence spectra of lumichrome ($A_{385} \sim 0.8$) in ethanol at 298 K, $\lambda_{ex} \sim 349$ nm. Curves a, -1.1; b, 0; c, 1.1; d, 2.2; e, 3.3 ns. (A) 0% acetic acid. (B) 5% (0.83 M) acetic acid. (C) 10% (1.67 M) acetic acid. (D) 20% (3.33 M) acetic acid.

Results

As has been shown earlier,[3] acetic acid catalyzes the phototautomerism of **1** in ethanol. The corrected fluorescence spectrum of **1** as a function of acetic acid concentration clearly yields an isoemissive point at 487 nm (Figure 2), indicating an excited-state equilibrium between the two tautomers, **1*** and **2***, emitting maximally at 447 and 545 nm (compared to 440 and 540 nm in dioxane), respectively.

Ethanol itself cannot act as a proton-transfer catalyst (general base) for the phototautomerism, as there is no evolution of the fluorescence of **2** in absolute ethanol (Figure 3A). With increasing acetic acid concentration, however, the 545-nm emission grows in intensity at the expense of the 447-nm emission. This is also shown by the steady-state fluorescence measurements (Figure 4). The slope of the plot shown in Figure 4 is 1.04 M^{-1}, which com-

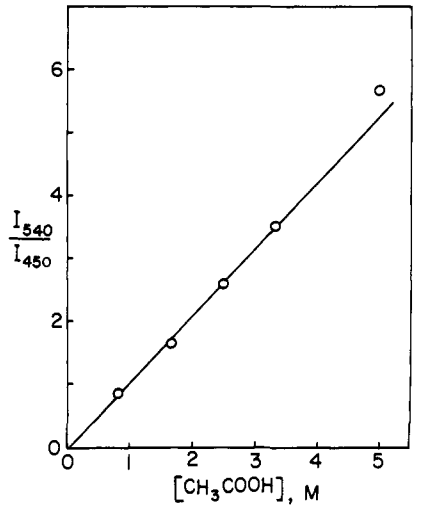

Figure 4. Ratios of I_f at 540 nm to I_f at 450 nm as a function of acetic acid concentration in ethanol at 298 K, slope = 1.04 M^{-1}.

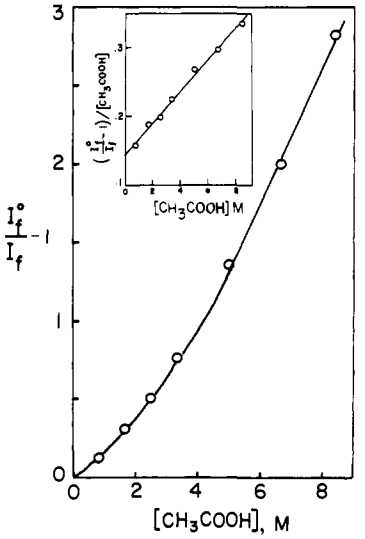

Figure 5. The Stern–Volmer plot for the lumichrome fluorescence (447 nm) in ethanol as a function of acetic acid concentration at 298 K. Inset shows a linear relationship.

pares with the value of 2.3 M^{-1} in pyridine (see later). The Stern–Volmer plot for the 447-nm emission shows a positive deviation at high acetic acid concentration (Figure 5). The K_{SV} values range from 0.12 to 0.17 M^{-1}, depending on the acid concentration range used.

Figure 6 presents fluorescence spectra of lumichrome as a function of pyridine concentration showing variations of two fluorescence band maxima, one at 440 nm due to **1*** and another at 540 nm due to **2***.[3] The fluorescence decay of **1** at 440 nm in dioxane was too short (<2 ns) to be deconvoluted reliably. However, the 540-nm emission decays much slower than the 440-nm emission, yielding a fluorescence lifetime of 10 ± 1 ns (phase shift value 8.8 ± 0.7 ns). The 540-nm fluorescence arises from the excited singlet state of **1**. As required, the corrected excitation spectra with respect to both emissions are identical with the absorption spectrum of **1** within experimental errors due to front-surface imprisonment and self-absorption effects.

A series of nanosecond time-resolved fluorescence spectra of **1** in dioxane as a function of pyridine concentration showed spectra similar to those shown in Figure 3. Very little emission at 540 nm evolved during 3 ns after pulse excitation of **1** in 0 and 1% pyridine–dioxane mixtures. However, the 540-nm emission grew with increasing pyridine concentration. In fact, at high pyridine concentrations, the 540-nm emission became predominant.

As shown in Figure 6, the 540-nm emission increases in intensity with pyridine concentration at the expense of the 440-nm emission.

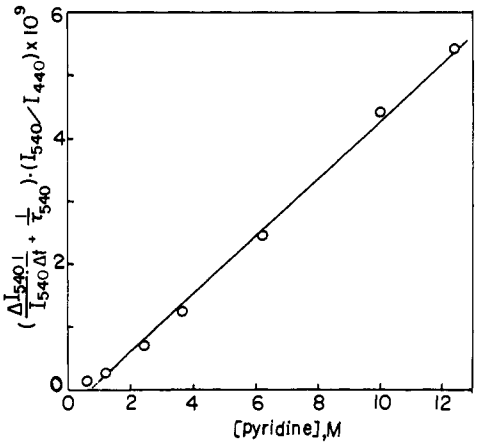

Figure 6. The dependence of derivative-intensity data from the time-resolved spectra of lumichrome (see text) on the pyridine concentration in dioxane at 298 K, slope = 4.5×10^8 M^{-1} s^{-1}, $\Delta I_{540} = I_{550(1.1ns)} - I_{540(0ns)}$ for Δt = 1.1 ns, $I_{540} = I_f$ at 0 ns, and τ_{540} = lifetime for the emission at 540 nm.

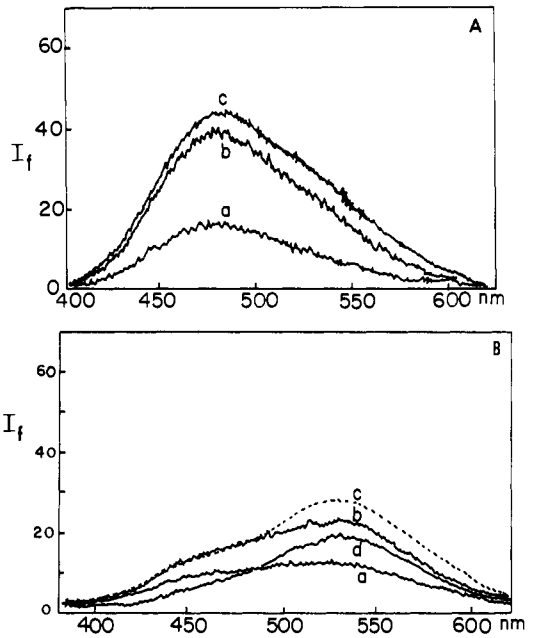

Figure 7. The time-resolved fluorescence spectra of lumichrome (A_{385} ~ 0.8) in water at 298 K, λ_{ex} ~349 nm. Curves a, −1.1; b, 0; c, 1.1; d, 2.2 ns. (A) pH 2.2. (B) pH 11.5.

This can also be shown by steady-state fluorescence ratios of these two emission bands (cf. Figure 4), as the quenching of the 440-nm emission follows the Stern–Volmer kinetics analogous to that shown in Figure 5. The quenching constant, K_{SV} = 0.2 M^{-1}, can be calculated from the slope of the Stern–Volmer plot.

The phototautomerism of **1** has also been examined in aqueous solution by the time-resolved fluorescence method. The spectra are recorded at three different pHs (2.2, 5.53, and 11.5). At pH 2.2, neither the N_1 nor N_3 proton is expected to dissociate, as pK_a values involved are pK_a^* = 3.6 (N_1) and 7.5 (N_3) and pK_a = 8.28 (for monoanion) and 12.9 (dianion).[5] At pH 5.53, the N_1 proton dissociates in the excited state, while both the N_1 and N_3 protons dissociate in the excited state at pH 11.5.

Figure 7A shows the time-resolved fluorescence spectra of **1** at pH 2.2, with the emission maximum at 482 nm. As expected, no significant **2** fluorescence evolves within 2.2 ns. This is also true at pH 5.53 (spectra not shown), where the N_1 proton should dissociate in the excited state of **1** with water acting as the general base. Only at pH 11.5, a longer wavelength fluorescence (maximum at 532 nm) is resolved in the nanosecond time scale (figure 7B). This emission is most likely due to an anionic form of **2** (the N_1 monoanion of **2** is equivalent to that of **1**).

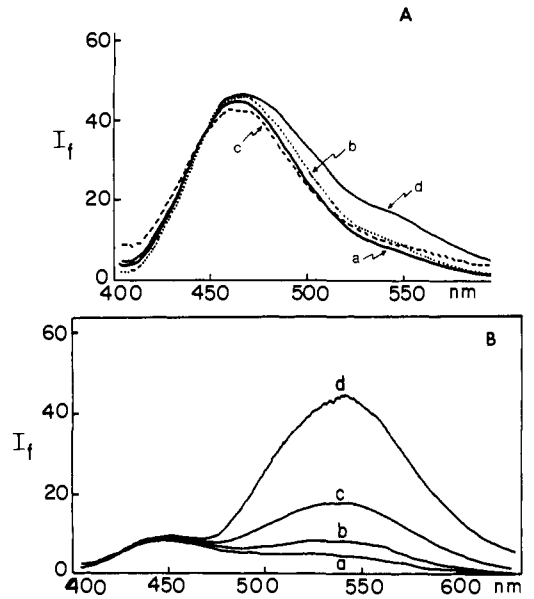

Figure 8. The time-resolved fluorescence spectra of lumichrome (A_{385} ~ 0.76) in 20% pyridine–dioxane, λ_{ex} ~349 nm. Curves a, -1.1; b, 0; c, 1.1; d, 2.2 ns. These spectra were normalized with respect to the intensity at 440 nm. (A) Temperature 100 K. (B) 270 K.

The phototautomerism of **1** depends on viscosity and temperature.[3,5] The time-resolved fluorescence spectra of **1** in 20% pyridine–dioxane at 100 K show a slow growth of the **2** fluorescence after 2.2 ns (Figure 8, curve d). However, the **2** fluorescence is clearly resolved at 270 K, even though the matrix at this temperature is still a frozen snow (Figure 8). Steady-state fluorescence measurements indicated that the phototautomerism occurred efficently at temperatures >133 K.[3]

Discussion

In the absence of pyridine or acetic acid, **1** absorbs a quantum of light and emits at 440–450 nm. However, in the presence of pyridine, for example, the 7,8-dimethylalloxazine (**1**) absorption spectrum remains unchanged, while a yellow fluorescence evolves with a maximum at 540 nm; the latter is attributable to the isoalloxazine tautomer (**2**).[3] In addition, the Stern–Volmer plot of **1** as a function of pyridine concentration in dioxane exhibited a straight line. At higher concentrations of acetic acid, however, the Stern–Volmer plot in ethanol deviates positively. However, a modified plot shown in Figure 5 (inset) yields a reasonable straight line. This behavior is indicative of ground-state complex formation.[10,11]

A log–log plot of fluorescence quantum yield ratio ϕ_1/ϕ_2 against pyridine concentration, according to Birks,[10] yielded a straight line, the slope (=1.03 with r^2 = 1.00) being the stoichiometry of the quenching reaction of **1***, i.e., 1:1 stoichiometry of **1*** and pyridine. A plot of I_{545}/I_{440} against pyridine concentration yielded a straight line with slope of 2.3 M^{-1}, thus confirming a 1:1 stoichiometry.

Steady-state and time-resolved fluorescence of **1** in the presence of acetic acid (cf. Figures 2–5) can be interpreted in terms of the simple kinetics of Scheme I, although the curvature of Figure 5 indicates that this scheme does not entirely account for ground-state complexes. The ground-state tautomer **2** is themodynamically unstable and rapidly reverts back to **1**, although it can be spectroscopically detected in viscous media such as in 5% pyridine–glycerol.[3]

For Scheme Ia, the following expression for the rate ratios of fluorescence from **1*** and **2*** can be derived:

$$I_{545}/I_{447} \simeq I_{540}/I_{450} = (k_5/k_1)(k_3/k_4 + k_5 + k_6)[CH_3COOH] \quad (1)$$

Scheme I

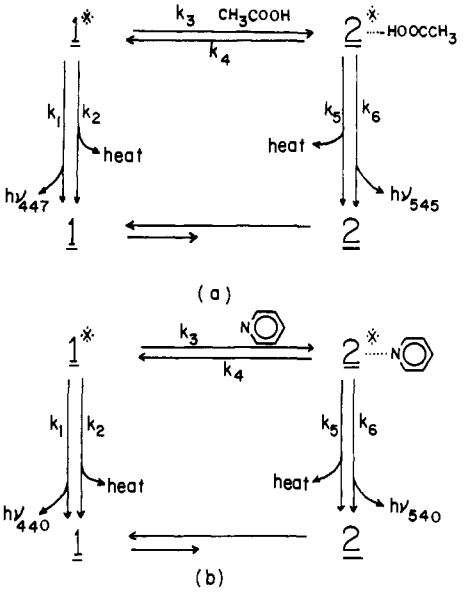

From the slope (=1.04) of the plot shown in Figure 4, the fluorescence lifetime (=2.65 × 10^{-9} s = $[k_4 + k_5 + k_6]^{-1}$) of **1** in acetic acid where the fluorescence is almost exclusively from **2*** (spectrum not shown) and k_5/k_1 = 0.99, we obtain $k_3 = 4 \times 10^8$ M^{-1} s^{-1}. From the K_{SV} value of 0.12 (Figure 5), we also obtain $k_4 = 3 \times 10^8$ s^{-1}.

The time-resolved fluorescence data (Figure 3) can be treated by the method of instantaneous derivative-intensity plot[12] to calculate k_3 and k_4, according to the equation

$$\left[\frac{(\Delta I_{545}/\Delta t)}{I_{545}} + (k_4 + k_5 + k_6)\right]\frac{I_{545}}{I_{447}} = k_3 f[CH_3COOH] \quad (2)$$

where $\Delta I_{545} = I_{545}(t_2, \text{ns}) - I_{545}(t_1, \text{ns})$, $\Delta t = t_2 - t_1$, I_{545} and I_{447} are fluorescence intensities (normalized to the constant excitation pulse intensity) at 545 and 447 nm, respectively, and

$$f = \left(\frac{[1^*]}{[2^*]} \Big/ \frac{I_{447}}{I_{545}} \simeq 0.52\right)$$

is the proportionality factor[12] for the conversion of I_{447} and I_{545} to the concentrations [**1***] and [**2***].[13] From a plot according to eq 2, k_3 can be calculated to be 3.1 × 10^8 M^{-1} s^{-1}. The slope of derivative-intensity plot shown in Figure 9 yields $k_4 = 2.8 \times 10^8$ s^{-1}. These values are in satisfactory agreement with the steady-state values, within experimental errors.

Steady-state and time-resolved fluorescence of **1** in the presence of varying concentrations of pyridine can be interpreted in terms of Scheme Ib. Using the slopes of 2.3 and 0.2 M^{-1} from plots of I_{545}/I_{440} vs. pyridine concentration and the corresponding Stern–Volmer relation, respectively, and with the fluorescence lifetime of 1.2 ns in dioxane, values of $k_3 = 3.3 \times 10^8$ M^{-1} s^{-1} and $k_4 = 6.9 \times 10^7$ s^{-1} are obtained, respectively.

For Scheme Ib, a derivative-intensity relation is shown in Figure 6. The slope yields $k_3 f = 4.5 \times 10^8$ M^{-1} s^{-1}, which compares closely with the value obtained in ethanol (vide supra). These values are an order of magnitude less than the diffusion-limited rate constant, $k_{diff} = 5.5 \times 10^9$ M^{-1} s^{-1}, under our experimental conditions

(10) Birks, J. B. "Photophysics of Aromatic Molecules"; Wiley-Interscience: New York, 1970; pp 442–443.

(11) We acknowledge a referee's comment regarding this point.

(12) Loken, M. R.; Hayes, J. W.; Gohlke, J. R.; Brand, L. *Biochemistry* **1972**, *11*, 4779.

(13) This value was taken as the ratio of amplitudes of fluorescence decay curves at 447 (lumichrome) and 545 nm (lumiflavin) in ethanol, under identical measuring conditions, i.e., same absorbances with intensity-normalized excitations at 349 nm and with an approximately constant-response PM tube (EMI 9817) at 447 and 545 nm. Since the natural lifetime and instrumental sensitivity factors are essentially identical for ethanol and dioxane solutions and the only major difference is a nearly twofold increase in ϕ_2 (lumiflavin) in dioxane, we may use $f \sim 1$ for an approximate estimate of k_3.

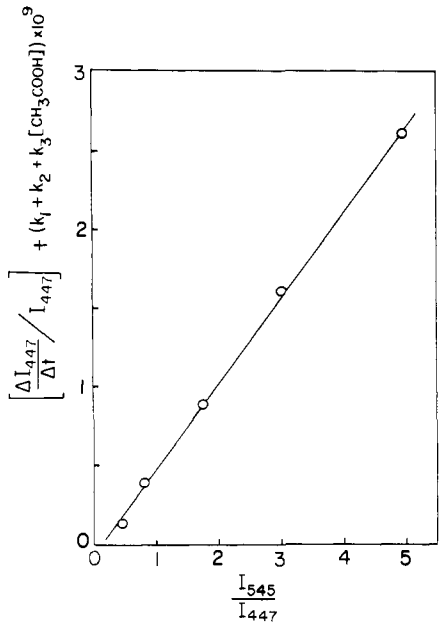

Figure 9. A derivative-intensity plot of time-resolved kinetic parameter, according to the equation $((\Delta I_f/\Delta t)/I_f) + (k_1 + k_2 + k_3[CH_3COOH]) = (k_4/f)(I_{545}/I_{447})$, as a function of acetic acid concentration at 298 K for lumichrome in ethanol.

(dioxane). Although we have not deconvoluted the rise time of **2***, the above values of k_3 are consistent with the slower rise time of **2*** than the excitation pulse rise time, assuming $f \sim 1$.[13]

The fact that the fluorescence of **2*** is not resolved within the nanosecond range examined (Figure 7) in aqueous solution of **1** at pH 5.53 [this pH being lower than $pK_a^*(N_1) = 3.6$][5] suggests that the photodissociation of the N_1 proton in aqueous solution is substantially slower than is the phototautomeric transfer of the proton from N_1 to N_{10} in dioxane and ethanol in the presence of pyridine and acetic acid, respectively. For 2-naphthol in water, photodissociation shows rate constants ranging from 4.1×10^7[14] to 5.1×10^7 s^{-1}.[12] Furthermore, the temperature dependence of the time-resolved fluorescence due to **2*** (Figure 8) suggests that the phototautomeric proton transfer is strongly viscosity dependent, in contrast to the dissociation of proton and the resulting ion-pair formation between N_1^- and the conjugated acid (pyridinium cation) in the excited state of **1**. The long-wavelength fluorescence of **1** at pH 11.5 (Figure 7) is probably due to a ca. 1:1 mixture of N_1 and N_3 anions.[5,15]

Conclusion

The nanosecond time-resolved fluorescence spectra of lumichrome in dioxane and ethanol in the presence of pyridine and acetic acid, respectively, have been obtained by a PAR boxcar averaging system. Inspection of these spectra strongly suggests that the excited lumichrome (**1***) undergoes a tautomeric proton shift from N_1 to N_{10}, yielding the excited flavinic tautomer (**2***) which emits maximally at 540–545 nm. Both steady-state and time-resolved fluorescence data yield rate constants of $3–4.5 \times 10^8$ M^{-1} s^{-1} for the phototautomeric reaction, and these rate constants are an order of magnitude lower than diffusion-controlled processes. The driving force for the phototautomeric proton shift is the redistribution of the electron density at N_1 and N_{10} upon excitation of lumichrome.[3] A strong temperature dependence, and that the photodissociation of the N_1 proton is substantially slower at neutral and acidic pHs than is the phototautomerism in dioxane and ethanol in the presence of pyridine and acetic acid, respectively, has been observed.

Acknowledgments. We are grateful to Professor S. Georgiou for his valuable advice in constructing the nanosecond time-resolved spectrofluorometer used in this work. Funds for the construction of this equipment were provided by the Dean of the College of Arts and Sciences, Texas Tech University.

(14) Weller, A. *Prog. React. Kinet.* **1961**, *1*, 187.
(15) Lasser, N.; Feitelson, J. *Photochem. Photobiol.* **1977**, *25*, 451.

Organic Photochemistry with 6.7-eV Photons: Photoisomerization of Tricyclo[3.2.1.$0^{2,4}$]oct-6-ene (Endo and Exo) and Tricyclo[3.2.2.$0^{2,4}$]non-6-ene (Endo and Exo)

R. Srinivasan,*[1a] Jose A. Ors, Karen H. Brown, Thomas Baum, Lloyd S. White, and Angelo R. Rossi*[1b]

Contribution from the IBM Thomas J. Watson Research Center, Yorktown Heights, New York 10598, and Chemistry Department, The University of Connecticut, Storrs, Connecticut 06268. *Received October 26, 1979*

Abstract: Photolysis of the title compounds at 185 nm in solution leads to internal addition of the olefinic group to the cyclopropane ring and cleavage of the cyclopropane to a bicyclic 1,4-diene. A theoretical analysis of the interactions between the π-orbitals of the double bond and the σ orbitals of the cyclopropane in each of these compounds has been carried out. The effect of through-bond interactions superimposed upon the through-space effects when extended to the valence excited states gives rise to three low-lying excited states which are (in order of decreasing energy) $\sigma_A \rightarrow \sigma_A^* + \pi^*$ (forbidden), $\sigma_S + \pi \rightarrow \pi^* + \sigma_A^*$ (allowed), and $\pi - \sigma_S \rightarrow \pi^* + \sigma_A^*$ (allowed). The internal addition reaction is identified with the $\pi - \sigma_S \rightarrow \pi^* + \sigma_A^*$ state and the cleavage of the cyclopropane to yield a 1,4-diene with the $\sigma_S + \pi \rightarrow \pi^* + \sigma_A^*$ state. The low reactivity of the *endo*-tricyclo[3.2.2.$0^{2,4}$]non-6-ene is believed to relate to a departure from the ordering of the excited states as described above.

Introduction

The tricyclic compounds **1**–**4** which incorporate an allylcyclopropane function in a rigid tricyclic framework have been of interest to both spectroscopists and photochemists. The interactions between the π electrons of the double bond and the Walsh orbitals of the cyclopropane have been examined in **1**, **2**, and **3** by photoelectron (PE) spectroscopy by Heilbronner and his coworkers[2] and by Bruckmann and Klessinger.[3] These workers

0002-7863/80/1502-5297$01.00/0